Electrochemical Study of Doxorubicin Interaction with Different Sequences of Single Stranded Oligonucleotides, Part I

David Hynek[1,2], Ludmila Krejcova[1,2], Ondrej Zitka[1,2], Vojtech Adam[1,2], Libuse Trnkova[2,3,4], Jiri Sochor[1,2], Marie Stiborova[5], Tomas Eckschlager[6], Jaromir Hubalek[1,2,7] and Rene Kizek[1,2,7,]*

[1] Department of Chemistry and Biochemistry, Faculty of Agronomy, Mendel University in Brno, Zemedelska 1, CZ-613 00 Brno, Czech Republic, European Union
[2] Central European Institute of Technology, Brno University of Technology, Technicka 3058/10, CZ-616 00 Brno, Czech Republic, European Union
[3] Department of Chemistry, and [4] Research Centre for Environmental Chemistry and Ecotoxicology, Faculty of Science, Masaryk University, Kotlarska 2, CZ-611 37 Brno, Czech Republic, European Union
[5] Department of Biochemistry, Faculty of Science, Charles University, Albertov 2030, CZ-128 40 Prague 2, Czech Republic, European Union
[6] Department of Paediatric Haematology and Oncology, 2nd Faculty of Medicine, Charles University and University Hospital Motol, V Uvalu 84, CZ-150 06 Prague 5, Czech Republic, European Union
[7] Department of Microelectronics, Faculty of Electrical Engineering and Communication, Brno University of Technology, Technicka 3058/10, CZ-616 00 Brno, Czech Republic, European Union
*E-mail: kizek@sci.muni.cz

Doxorubicin is a known anticancer drug intercalating into dsDNA. The mechanism of interaction of doxorubicin with ssDNA is not clear. In this study, adsorptive transfer stripping technique coupled with square wave voltammetry was used for studying of interaction of doxorubicin with single stranded oligonucleotides (ssODN) in various ratios (1:1, 1:2 and 1:5) and interaction times (0-300 min.). When comparing the results for three ratios of the mixture between drug and ssODN we found that the interval of peak intensities of oligonucleotide reduced with the increasing ratio of oligonucleotide-doxorubicin, i.e. for ratio 1:1 it is 25-85 %, for ratio 1:2 it is 16-60 % and for ratio 1:5 it is 19-51 %. The interval of relative signal intensities of doxorubicin ranges from 8 to 100 % for ratio 1:1, 22-100 % for ratios 1:2 and 1:5. The results showed the assumption that DOXO peak height increased with increasing concentration of the drug intercalated into ssODN, but the signals CA peaks changes during the interaction suggest the changes in the structure of ssODN.

Keywords: intercalating drug; doxorubicin; hetero-nucleotides; square wave voltammetry; adsorptive transfer stripping technique; DNA

1. INTRODUCTION

Cancer is a very serious health problem in all developed countries. Since the beginning of the 21st century cancer becomes one of the most common primary cause of death, of which malignant breast tumours predominate for women [1-3] and prostate cancer in men. [4-6]. Treatment options are based on surgical removal of cancerous tissue, radiotherapy and chemotherapy. Chemotherapy approaches interfere with quite different cellular and molecular processes. Intercalators belong to the important group of drugs that are used in cancer therapy. Platinum derivatives [7-12] followed by anthracyclines and taxanes [13,14] belong to the oldest and still most widely used drugs of this mechanism.

1.1 Doxorubicin

Doxorubicin ((8S,10S)-10-(4 - amino - 5 - hydroxy - 6 - methyl - tetrahydro - 2H - pyran - 2 - yloxy) - 6,8,11 – trihydroxy – 8 - (2-hydroxyacetyl)-1-methoxy-7,8,9,10-tetrahydrotetracene-5,12-dione) called also as daunomycin and/or adriamycin is an anthracycline antibiotic. The first anthracyclines were isolated from the pigment-producing *Streptomyces peucetius* early in the 1960s and were named doxorubicin or hydroxyldaunorubicin (trade name Adriamycin) [15]. Nowadays, it is commonly used in the treatment of a wide range of cancers. The exact mechanism of action of doxorubicin is complex and still somewhat unclear, though it is thought to interact with DNA by intercalation and topoisomerase II inhibition [15].

1.2 Biological effect of doxorubicin

Kiyomia et al. performed some experiments to clarify the intracellular specificity of the differential cytotoxic effects of doxorubicin on neoplastic and normal cells. These results suggest that doxorubicin exerts cytostatic effects on neoplastic and normal undifferentiated cells through the inhibition of DNA synthesis by DNA intercalation, and cytotoxic effects on neoplastic cells through the accumulation of reactive oxygen species resulting from low scavenger enzyme activities. The cytotoxic effects on normal differentiated cells may be related to the high levels of production of reactive oxygen species due to high mitochondrial NADH-cytochrome c reductase activity [16]. Doxorubicin is commonly used to treat some leukaemias, Hodgkin's and non- Hodgkin's lymphomas, as well as cancers of the bladder, breast, stomach, lung, ovaries, thyroid, soft tissue and bone sarcomas, multiple myeloma, and others.

1.3 DNA interactions with doxorubicin

Doxorubicin is known to interact with DNA by intercalation and inhibition of macromolecular biosynthesis. This inhibits the function of the enzyme topoisomerase II, which unwinds DNA for transcription. Doxorubicin stabilizes the topoisomerase II complex after it has broken the DNA chain

for replication, preventing the DNA double helix from being resealed and thereby stopping the process of replication. The planar aromatic chromophore portion of the molecule intercalates between two base pairs of the DNA [17], while the six-membered daunosamine sugar sits in the minor groove and interacts with flanking base pairs immediately adjacent to the intercalation site, as evidenced by several crystal structures.

1.4 Reactive oxygen species generation by doxorubicin and its cardiotoxicity

Generating of reactive oxygen species causing lipoperoxidation that cause damaging of cell membranes, apoptotic changes via interaction with iron ions and activation of NFκB belongs to the other important effect of doxorubicin *in vivo* [15,18]. The scheme of the effects of the generated radicals is shown in Fig. 1. Anthracyclines including doxorubicin have long been said to induce cardiotoxicity by mechanisms other than those mediating their antitumor effectiveness, a concept which has raised hopes to design strategies for protecting the heart while not diminishing tumour response. Here we describe the most recent advances that may help to shed light into the mechanisms by which anthracyclines induce cardiotoxicity in experimental or clinical settings [15,19]. To reduce their cardiotoxicity, nanoparticles based approaches for encapsulation of these drugs seems to be very convenient for this purpose [20].

1.5 Electrochemistry of doxorubicin

1.5.1 Electroanalytical detection of doxorubicin

There is paid great attention to electrochemistry of doxorubicin and related drugs due to considerable electroactivity of these molecules [22-34]. Doxorubicin is complex molecule, where both quinone and hydroquinone groups are electroactive and can be used to identify electrochemical reduction and/or oxidation of the drug (Fig. 1). Studies have been carried with mercury, carbon and other types of modified electrodes. *Mercury electrodes*. The redox process presents two sets of reduction waves, corresponding to the reduction of the quinone group and the carbonyl side chain, respectively [35]. Polarographic behaviour of doxorubicin has been investigated by several authors with good sensitivity [23,36-39]. Recently published paper used voltammetry with linear scan and chronopotentiometric stripping with constant current for the analysis of doxorubicin. The chronopotentiometric stripping with constant current method was also applied to monitor the doxorubicin interaction with double- (ds) and single-stranded (ss) DNA [40]. Besides this, adsorptive transfer technique can be also utilized for interactions studies between biologically active species and drug [41]. *Carbon paste electrodes*. Basic electrochemical behaviour of doxorubicin at carbon paste electrode (CPE) was described in the beginning of eighties of the last century [42] followed by several other papers [43-47]. In addition, it was shown that preconcentration and quantitation of doxorubicin could be achieved via a flow-injection approach utilizing adsorption of the drug onto a CPE, medium exchange, and differential pulse voltammetry on the adsorbing surface. It was possible to determine the drug in urine by direct injection of the sample with no preliminary steps required. The sensitivity,

linearity, and selectivity of the flow injection approach were markedly improved relative to the earlier batch method in which the adsorption step was done in a stationary sample solution [48].
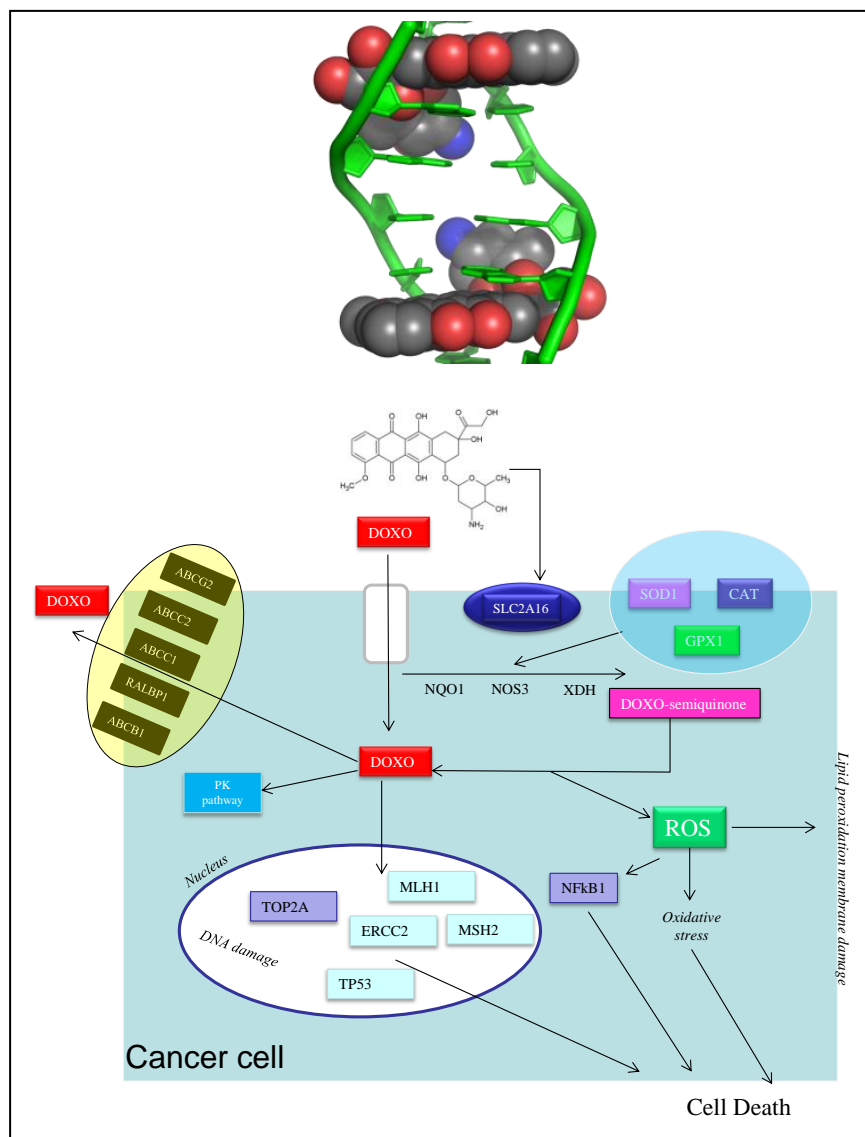

Figure 1. Scheme of doxorubicin interactions with different proteins in cancer cell., ABCB1 (ATP-binding cassette, sub-family B (MDR/TAP), member 1), RALBP1, ABCG2, ABCC2 (ATP-binding cassette, sub-family C (CFTR/MRP), member 2), ABCC1 (ATP-binding cassette, sub-family C (CFTR/MRP), member 1): cell transporters responsible for resistance; DOXO: doxorubicin; enzymes forming doxorubicin-semiquinones radicals: CAT, GPX1, NQO1(NAD(P)H dehydrogenase, quinone 1), NOS3 (nitric oxide synthase 3 (endothelial cell)), SOD1, XDH (xanthine oxidase). ROS: reactive oxygen species. Transcription factor NFκB1, activation NFκB blocked apoptocic cell death. TOP2A topoisomerase II. MSH2, MLH1 reparation genes, TP53 and ERCC2 have been shown to functionally interact in a p53-mediated apoptotic pathway. SLC22A16: organic cation/carnitie transporter, member 16. Adopted and modified according to [21].

Other types of the electrodes. The variations in the cyclic voltammetric behaviour of doxorubicin in an aqueous medium on addition of DNA were studied and utilized for the quantitation of DNA using rotating disk electrode. The peak current of doxorubicin decreased considerably after intercalating to the large, slowly diffusing DNA, and the apparent diffusion coefficients of doxorubicin and doxorubicin-DNA adduct were determined [49]. Ni/glassy carbon ion implantation modified electrode as working electrode was used for detection of doxorubicin by linear sweep voltammetry [50,51]. In addition, it was shown that bismuth bulk electrodes are very convenient for sensitive adsorptive stripping voltammetric determination of the drug doxorubicin [52]. A novel COOH[+] ion implantation-modified indium oxide (COOH/ITO) electrode was prepared and applied for determination of doxorubicin. The selectivity of the electrode was illustrated by determination of doxorubicin in urine samples [53]. The poly-L-glutamic as a biodegradable acid was used polymer conjugated to doxorubicin for modification glassy carbon electrode. The interaction was done via terminal amino groups of the drug and the side chain carboxyl groups of branched poly-L-glutamic acid film. This approach can be used as the base to develop a simple voltammetric sensor for the determination of doxorubicin in human urine [54].

1.5.2 Interaction of doxorubicin with DNA; Hybridization biosensor

The investigations of drug-DNA interactions would provide new compounds to be tested for an effect on a biochemical target, and also to be used as promising hybridization indicators for the design of DNA biosensors, which will further become DNA microchip systems. An overview on DNA biosensors based primarily on drugs interacting with DNA showing how to determine this interaction electrochemically, the quantification of drug and/or DNA, and the promising applications of these drugs as DNA hybridization indicator was published [55,56]. Interactions between DNA-intercalating molecules, methylene blue and doxorubicin, and gold surface modified by various DNA species and n-hexadecyl mercaptan were investigated by cyclic voltammetry. The presence of ssDNA and dsDNA in the monolayer facilitated the redox reaction of methylene blue and doxorubicin on the modified electrode. Both methylene blue and doxorubicin diffuse along the ssDNA in the ssDNA-containing monolayers, and they additionally intercalate into the dsDNA in the dsDNA-containing monolayers. No sufficient evidence was shown to indicate that an organized monolayer was formed by the thiol-labelled dsDNA on gold surface, and that the redox reactions of methylene blue and doxorubicin were carried out by electron transfer through DNA helix [57]. Doxorubicin intercalation and *in situ* interaction with double helix DNA was investigated using a voltammetric DNA-biosensor. Oxidation and reduction of doxorubicin molecules intercalated in double helix DNA were investigated in order to understand the *in vivo* mechanism of action with this anti-neoplasic drug. The results showed that the interaction of doxorubicin with DNA is potential-dependent causing contact between DNA guanine and adenine bases and the electrode surface such that their oxidation is easily detected. A mechanism for doxorubicin reduction and oxidation in situ when intercalated in double helix DNA immobilised onto the glassy carbon electrode surface is presented and the formation of the mutagenic 8-oxoguanine explained [58].

Detailed electrochemical study of interaction doxorubicin with DNA was performed by Vacek et al. on carbon pyrolytic graphite (PGE) [40]. Doxorubicin adsorbed at the PGE surface produced two pairs of reversible signals; one at -0.5 V (anodic and cathodic peaks) corresponding to the Q group I and the other around +0.5 V corresponding to the QH_2 group II. Both electrode processes are related to the Q/QH_2 redox pairs: $Q + 2e^- + 2H^+ \leftrightarrow QH_2$ [40]. Sodium 1,4-dihydroxy-9,10-anthraquinone-2-sulphonate (Na-Qz-2S) is a molecule that resembles anthracycline drugs and has a simpler structure in comparison to these drugs. Two electrons in the course of chemical action reduce this molecule like the anthracyclines. Electrochemical methods were used to identify this process. UV-Vis and fluorescence spectroscopy were used to analyse binding of the compound to calf thymus DNA. The binding constant and site size were evaluated for Na-Qz-2S and the same compared to that of the anthracyclines. Such comparisons are essential in order to understand whether the simpler hydroxy-anthraquinones can be a substitute for anthracycline drugs in cancer chemotherapy [59]. This topic attracts more attention as it can be well documented by several papers devoted to the electrochemical studies of DNA-doxorubicin behaviour [60-62]. There are suggested various electroanalytical approaches to investigate the interactions of doxorubicin with ssDNA and/or dsDNA. It clearly follows from the results obtained that doxorubicin intercalates into dsDNA and strongly interacts with ssDNA [40]. Detailed study of doxorubicin interactions with DNA *in vitro* and *in vivo* was performed by us using square wave voltammetry. Intercalated doxorubicin reduced observed dsDNA cytosine and adenine (CA) signal, but also provided new signal called DOXO at -0.35 V. This phenomenon was observed at both single and double stranded DNA standards. We also employed adsorptive stransfer stripping technique coupled with SWV for study of doxorubicin-DNA interactions. Doxorubicin intercalation into dsDNA molecule adsorbed onto working electrode was fast, because we observed considerable changes in CA and DOXO signals after 360 s. Finally, we detected doxorubicin-DNA adducts formed in doxorubicin treated neuroblastoma cells [63]. Other experimental results were presented in the following papers [64-68].

Besides interaction studies itself, doxorubicin was studied from the point of view to describe its cardiotoxic properties or as intercalator for testing of DNA hybridization sensors. The interaction of doxorubicin with Fe(III) ions and nicotinamide has been followed by square-wave voltammetry, cyclic voltammetry and UV-VIS spectroscopy techniques at aerobic and anaerobic conditions. Fe(III)-doxorubicin complex gives a 1-electron reversible step. Further, the Fe(III)-doxorubicin complex was found to be more stable at aerobic conditions. Because of the formation of this doxorubicin intermediate, nicotinamide may reduce the cardiotoxic effect of doxorubicin and cause to its detoxification [69]. Other authors report an electrochemical biosensor for the detection of short DNA oligonucleotide of the avian flu virus H5N1. To fabricate this DNA biosensor, a gold electrode surface was modified with thiolated DNA probes with a sequence complementary to the target DNA. This modified Au electrode was incubated in a buffer solution containing the target DNA to form double-stranded DNA through hybridization. The ds-DNA on the electrode surface was then labelled with silver nanoparticles conjugated with a well-known DNA intercalator, doxorubicin [70]. An electrochemical method for the detection of DNA damage by combining the layer-by-layer assembly film with doxorubicin as an electrochemical probe was developed. The layer-by-layer dsDNA/PEI film was prepared by the alternate adsorption of polycationic polyethyleneimine and negatively charged

natural DNA onto glassy carbon electrode surface. Its electrochemical behaviours were characterized by electrochemical impedance spectroscopy and differential pulse voltammetry, and the optimal value. DNA damage induced by styrene oxide was investigated and the promising results showed that the present method can be a useful tool for the detection of DNA damage [71].

1.5.3 Nanotechnology in doxorubicin analysis

A highly sensitive method for electrochemical detection of doxorubicin was proposed on the carbon nanotubes (CNT) modified electrode. The supramolecular interaction between the CNT and the anthracyclin could significantly enhance the electron transferability, which sharply increased the detection sensitivity and lowered the detection limit. It can be predicted that many more analogues could be monitored on such a platform with high sensitivity [72]. A novel carbon nanotubes modified glassy carbon electrode was simply and conveniently fabricated. The electrochemical properties of doxorubicin at the carbon nanotubes modified electrode were investigated, and two pairs of redox peaks were observed at the different potentials. Based on this, an ultrasensitive electrochemical method was proposed for the determination of doxorubicin. The analysis method is demonstrated by using urine samples obtained from cancer patients following intravenous administration of doxorubicin [73]. An electrochemical sensor has been constructed for the determination of doxorubicin that is based on a glassy carbon electrode modified with silver nanoparticles and multi-walled carbon nanotubes with carboxy groups. The modified electrode was characterized by scanning electron microscopy and exhibits a large enhancement of the differential pulse voltammetric response to doxorubicin [74]. The DNA-multiwalled carbon nanotube (MWCNT) bioconjugates were prepared by dispersing MWCNTs in calf thymus single-stranded or double-stranded DNA aqueous solution. The electrochemical behaviours of doxorubicin at ssDNA and dsDNA-MWCNT bioconjugates-modified glassy carbon electrodes were studied by cyclic voltammetry. The aromatic nucleotide bases in ssDNA interact with the sidewalls of MWCNTs via pi-stacking, leaving the deoxyribose backbones exposed to solution, which causes the surface of the MWCNT highly negatively charged [75]. Therefore, the interaction between doxorubicin and ssDNA-MWCNT was only electrostatic. In addition to electrostatic interaction, doxorubicin can interact with dsDNA through intercalating into base pairs and binding to minor grooves, which makes the electrochemical behaviour of doxorubicin at dsDNA-MWCNT different from that at ssDNA-MWCNT bioconjugates-modified GCEs [75]. A nanohybrid adduct of the widely used doxorubicin with single-walled carbon nanotubes (SWNTs) was prepared. Ultraviolet-visible-near infrared and fluorescence spectroscopy and electrochemistry of DM-functionalized SWNTs reveal that DM interacts with SWNTs through strong pi-pi stacking and there is a significant photo-induced charge-transfer interaction between the two components. Importantly, the novel adduct modified the glassy carbon (GC) electrode to give a much enhanced electrochemical activity than those of DM adsorbed onto not only the bare GC electrode but also the SWNTs-modified GC electrode [76]. A novel graphene oxide-doxorubicin hydrochloride nanohybrid (GO-DXR) was prepared via a simple noncovalent method, and the loading and release behaviours of doxorubicin on graphene oxide were investigated. The loading and release of doxorubicin on graphene oxide showed strong pH

dependence, which may be due to the hydrogen bonding interaction between graphene oxide and doxorubicin. The fluorescent spectrum and electrochemical results indicate that strong π- π stacking interaction exists between them [77]. Electroactive biotin ligands were prepared by the reaction of doxorubicin with biotinylating reagents with a different spacer. These biotin ligands exhibited similar electrochemical properties to those of doxorubicin, but the adsorptivity of the ligands on the electrode increased with increasing length of the spacer. The electrode response of these ligands decreased when specifically bound with avidin. This made it possible to detect electroinactive avidin indirectly. Biotin was detected by observing the competitive reaction between biotin and the ligands for the limited binding sites of avidin. The binding strength of the labelled biotins with avidin was compared with that of unlabelled biotin by using an enzyme assay [78,79]

A multi-walled carbon nanotubes MWCNT and cobalt nanoparticles modified indium tin oxide electrode (Co/CNT/ITO) was fabricated for the first time on an indium tin oxide electrode. The modified indium tin oxide electrode was characterized using cyclic voltammetry, scanning electron microscopy and energy dispersive spectroscopy [80]. A sensitive electrochemical method was developed for the determination of doxorubicin at a glassy carbon electrode modified with a nano-TiO_2/nafion composite film. The nano-TiO_2/nafion composite film modified GCE exhibited excellent electrochemical behaviour toward the reduction of doxorubicin [81]. Nano titanium dioxide (TiO_2)-modified electrodes facilitated the biorecognition of doxorubicin in the absence and presence of UV irradiation. The results demonstrated that the photovoltaic effect of the nano TiO_2-modified electrodes could enhance the DNA binding affinity and the detection sensitivity of the respective biomolecule recognition. Meanwhile, by using in situ electrochemical contact angle measurements, the hydrophobic- hydrophilic features of the target interface were observed to change remarkably when doxorubicin binds to DNA at the nano TiO_2-modified glassy carbon electrode under UV irradiation [82]. Gold nanoparticles were situated on the surface of glassy carbon electrode to form a gold nanoparticles modified electrode. The designed single-stranded RNA was immobilized on gold nanoparticles through a thiol linker as a probe RNA. Then, the complement stranded RNA, which can combine with the probe ssRNA to form a double-stranded RNA with a recognition unit of theophylline, was linked on the probe RNA through a hybrid reaction in the presence of theophylline. Doxorubicin was selected as an electrochemical indicator [83].

It can be concluded that nano-based materials in combination with electrochemistry belong to the promising tools in doxorubicin research. However, there is still lack in the understanding of the basic principles of doxorubicin action. Therefore, the main aim of this study was to investigate the interaction of doxorubicin with different sequences of single stranded oligononucleotides (dsODN) using electrochemistry.

2. EXPERIMENTAL PART

2.1 Chemicals

Doxorubicin was purchased from TEVA (Czech Republic). Sodium acetate, acetic acid, water and other chemicals were purchased from Sigma Aldrich (USA) in ACS purity unless noted otherwise.

Four types of oligonucleotides were from Sigma Aldrich (Table 1). Each of them had ten nucleotides with various sequences of bases. Standard solutions of the oligonucleotide (10 µg/ml) were prepared with ACS water and stored in dark at -20°C. The concentration of oligonucleotide was determined spectrometrically at 260 nm using spectrometer Specord 600 (Analytic Jena, Germany) in quartz cuvettes and thermostat carousel (20 °C). Pipetting was performed by certified pipettes (Eppendorf, Germany).

Table 1. Four types of single stranded oligonucleotides used in this study.

Name	Sequence	Name	Sequence	Name	Sequence	Name	Sequence
MT5	5´-CCAAGACAAA	CA3	5´-GCTAAAATCC	GL6	5´-AATGTTCCAT	GL4	5´-TTTTGTAAAC

2.2 Square wave voltammetric measurements

Electrochemical measurements were performed with AUTOLAB PGS30 Analyzer (EcoChemie, Netherlands) connected to VA-Stand 663 (Metrohm, Switzerland) and 797 VA computrace (Metrohm, Switzerland) using a standard cell with three electrodes. A hanging mercury drop electrode (HMDE) with a drop area of 0.4 mm^2 was employees the working electrode. An Ag/AgCl/3M KCl electrode served as the reference electrode. Pt electrode was used as the auxiliary electrode. For smoothing and baseline correction the software GPES 4.9 supplied by EcoChemie was employed. Square-wave voltammetric (SWV) measurements were carried out in the presence of acetate buffer pH 5.0. SWV parameters: potential step 5 mV, frequency 280 Hz, time of accumulation 120 s [63]. The analysed samples were deoxygenated prior to measurements by purging with argon (99.999 %), saturated with water for 120 s. All experiments were carried out at room temperature (25°C).

2.3 Preparation of deionised water and pH measurement

The deionised water was prepared using reverse osmosis equipment Aqual 25 (Czech Republic). The deionised water was further purified by using apparatus MiliQ Direct QUV equipped with the UV lamp. The resistance was 18 MΩ. The pH was measured using pH meter WTW inoLab (Weilheim, Germany).

2.4 Mathematical treatment of data and estimation of detection limits

Mathematical analysis of the data and their graphical interpretation was realized by software Matlab (version 7.11.). Results are expressed as mean ± standard deviation (S.D.) unless noted otherwise (EXCEL®). The detection limits (3 signal/noise, S/N) were calculated according to Long

and Winefordner [84], whereas N was expressed as standard deviation of noise determined in the signal domain unless stated otherwise.

3. RESULTS AND DISCUSSION

The importance of this paper lies in the studying of doxorubicin interaction with DNA structure for better understanding of electron transport on DNA [85,86] on the one side and for searching how to enhance therapeutic effects of doxorubicin (target drug delivery) and how to decrease cardiotoxicity of this drug [87-89].

3.1 The influence of ssODNs concentration on CA peak height

Studying of the influence on the applied concentration, accumulation time, supporting electrolyte, temperature or other physico-chemical conditions belong to the characteristic behaviour of DNA on the electrodes. In our experiment, we based on earlier published results and as a primary characteristic of the examined sequences, we chose ODN concentration. ssODNs were analysed using adsorptive transfer technique (described in details in Refs. No. [28,90-93]) coupled with square wave voltammetry (AdTS SWV). *Concentration dependence*. Dependencies were measured under standard laboratory conditions (temperature 20 °C, acetate buffer pH 5.00, 10 independent measurements was carried out for each sequence), concentrations ranging from 0.1 to 3.5 µg/ml oligonucleotide at the time of accumulation of 120 s on HMDE. To follow the changes in the voltammograms, redox peak of cytosine and adenine (CA peak) measured at -1.4 V (Table 2) was considered. Dependencies in the mentioned concentration intervals are shown in Fig. 2A for GL6, in Fig. 2B for GL4, in Fig. 2C for CA3 and in Fig. 2D for MT5. Primary sequence of studied ODNs was selected to change position of adenine as first and most expected target for doxorubicin (Table 1). The obtained curves are linear with the concentration range from 0.1 to 0.75 µg/ml with R^2 higher than 0.99 for studied ssODNs except CA3 showing $R^2 = 0.97$. Courses of concentration dependencies are of polynomial character (2nd degree polynomial) with a confidence value higher than 0.99 for each analysed ODN sequences in the interval from 0.1 to 3 µg/ml. MT5, which contained three adenines at the end and at the middle of the chain, gave the highest CA peaks. CA3 with four adenines in the middle of the chain gave the second highest CA peaks. Sequence GL4 and GL6 gave peaks of app. Similar heights, and both sequences contained three adenines. The intensity of the signal sequence depends on the number of adenine in the sequence, but does not depend on their position in the chain. Considering the peak of 3 µg/ml MT5 as 100 %, the CA peaks of other ssODNs at same concentration were as follows – GL4: 68 %, GL6: 71 % and CA3: 85 %. At 0.75 µg/ml, CA peaks of other ssODNs at same concentration were as follows – GL6: 81 %, GL4: 82 % and CA3: 84 %. It clearly follows from the results obtained that the differences between the heights of CA peak for each nucleotides (relative to maximum value) with decreasing concentration of the oligonucleotide. Besides peak heights, we were also interested in the issue how

primary structure of studied ssODNs influences peak potential. Location of the adenine in the oligonucleotide chain affects the position of the peak potential.
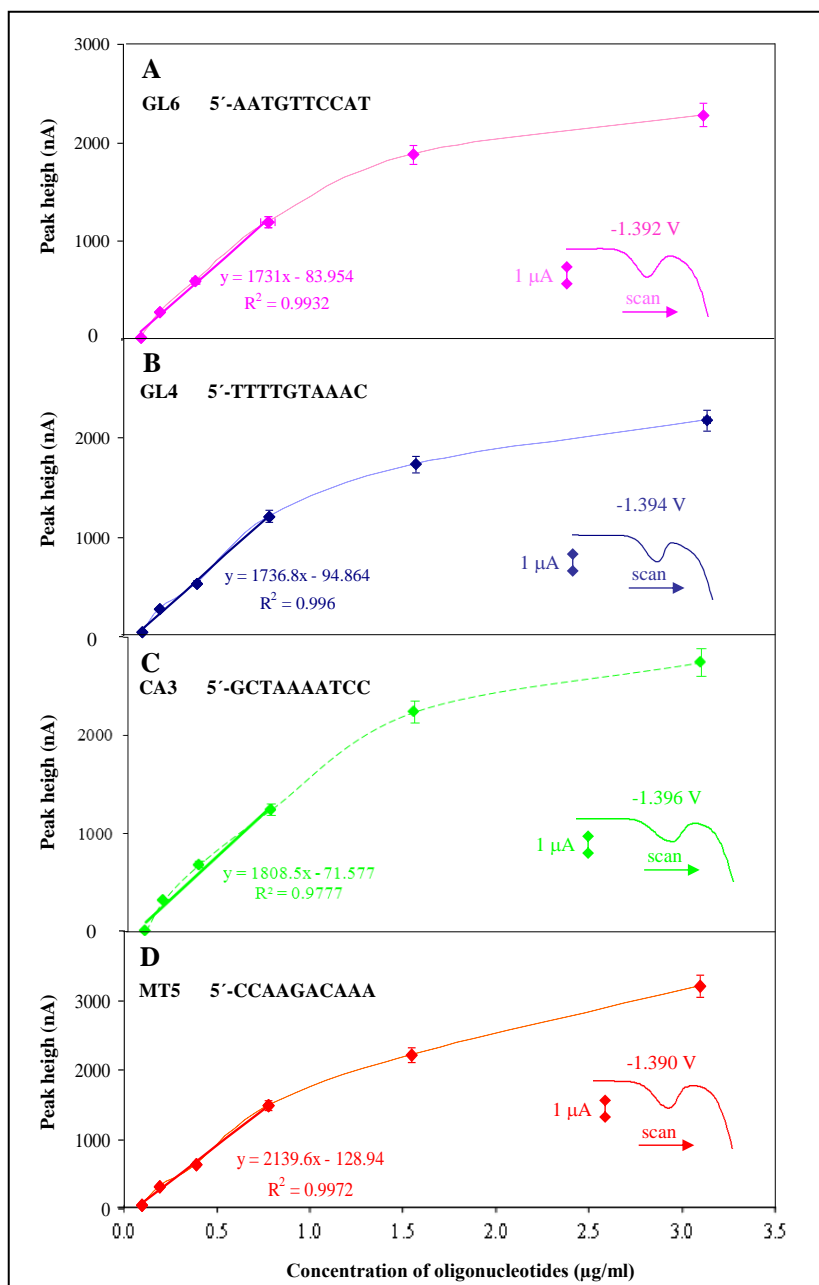

Figure 2. Dependences of ssODN ((**A**) GL6, (**B**) Gl4, (**C**) CA3 and (**D**) MT5) CA peak height on concentration. In the bottom inset in all figures, CA peak is shown. First four points of calibration curves have linear behaviour for each ssODNs. AdTS SW voltammetry: time of accumulation 120 s, potential step 5 mV, frequency 280 Hz. Number of measurement was 10.

The values of the detected potentials varied for individual sequences and increased in the following order as MT5 < GL6 < GL4 < CA3 (Table 2). Besides, we also compared slopes of the

linear part of concentration dependencies and found that GL4 and GL6 had similar slopes. CA3 with the primary structure as GCTAAAATCC showed higher slope. MT5 with adenines at the end of the chain had the highest slope. The issue of the impact of the sequence of bases in the ODN chain, the influence ionic strength and pH was investigated [94-96]. In addition to protonation/deprotonation, binding of ions into the structure of ODN play an important role in structural changes (harpins, cross-duplex) [94,97-99]. In the following experiments studying the effects of doxorubicin, concentration of 0.5 µg/ml ssODN (concentration in the middle of the linear curve) was chosen. CA peaks measured in ssODN with adenine at the end of the chain showed more negative potentials than those measured in ssODNs with adenine in the middle of the chain (Table 2).

Table 2. MT5, GL6, GL4 and CA3 single stranded oligonucleotides (concentration 5 µg/ml) used to measurement and potential CA peak on the acetate buffer pH 5.00. AdTS SW voltammetry: time of accumulation 120 s, potential step 5 mV, frequency 280 Hz. Number of measurement was 10.

CA peak	MT5	GL6	GL4	CA3
Potential (V)	1.390 ± 0.002	1.392 ± 0.002	1.394 ± 0.001	1.396 ± 0.002

3.2 SW voltammetric analysis of ssODNs interactions with doxorubicin

Typical SW voltammograms of GL6, GL4, CA3 and MT5 (0.5 µg/ml) measured in the acetate buffer pH 5 and time of accumulation 120 s are shown in Figs. 3A, B, C, and D, respectively. There are well developed CA peak at -1.4 V. However, the changes in the voltammograms were observed after addition of 2.5 µg/ml doxorubicin to the studied dsDNA (90 min., 400 rpm, 25 °C). These changes were expected due to the intercalation of doxorubicin into DNA. The marked decrease in CA peak height and one signal corresponded to doxorubicin called DOXO (-0.4 V) was observed (Fig. 3). Based on the published results it can be expected that there is still not very well explored physical interactions at the interface of DNA strand and doxorubicin. It is likely that these interactions indicate strong π-π stacking interaction between them [77]. One may speculate, which nucleic acid bases are involved in this interaction. This interaction is expected between guanosine and adenine, in a much lesser extent, cytosine or other irregular base (Fig. 4).

Based on the results shown in Fig. 3, the following experiment monitoring CA peaks of ssODN and reduction signals of doxorubicin was carried out. All measurements were done in triplicates. Primarily, we determined CA peak for all tested ODNs (0.5 µg/ml) without any addition of doxorubicin in the following times of incubation time of the interaction (15, 30, 45, 60, 90, 120, 150, 180, 210, 240, 270 and 300 min.). The CA peaks did not change with relative standard deviation lower than 5 % (n = 10) during the incubation. Therefore, this peak and its height were selected as a reference value and are shown in Fig. 5 as -▲-. The interactions of ssODN with doxorubicin caused marked decrease in CA peak height and appearance of signal of doxorubicin called DOXO. In general, behaviour of ssODNs was very different from those measured for dsODNs [100].
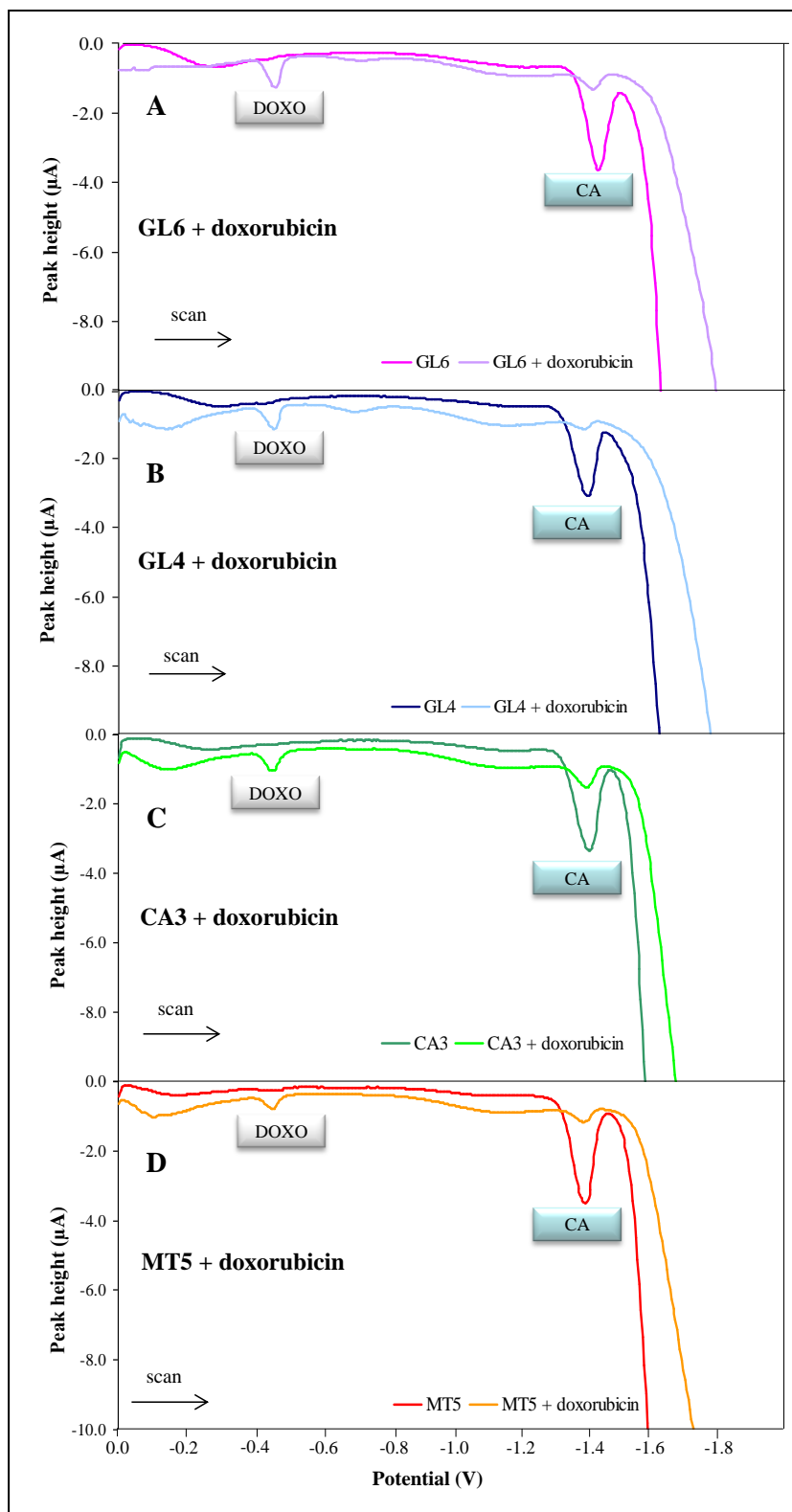
Figure 3. Typical SW voltammograms of (**A**) GL6d, (**B**) GL4d, (**C**) CA3d and (**D**) MT5d (0.5 μg/ml) and its mixture with doxorubicin (2.5 μg/ml). Time of interaction 90 min. Light curves correspond to mixtures of oligonucleotide and doxorubicin. Dark curves correspond to pure single-stranded oligonucleotides. Doxorubicin gave two peaks called "IC" and "OC". For other experimental details, see Fig. 1 and Tab. 2.

Three ratios of both substances were tested as follows: 1:1, 1:2 and 1:5 (doxorubicin: ssODN, concentration of ssODN was 0.5 µg/ml). In the case of GL4 and GL6 ssODNs, there are well distinguished all measured time dependencies for the tested ratios and for determined peak heights (CA and DOXO). **GL6.** CA peak decreased for more than 30 % (1:1(-♦-)) and for more than 50 % (1:2(-x-) and 1:5(-■-)) in the beginning of incubation. CA peak enhanced with the increasing time of incubation (Fig. 5A). DOXO peak increased with the increasing time of incubation, however, the most sharp increase was determined in 1:5 ratio, which shown on excess of doxorubicin, which is not bound in DNA (Fig. 5A).
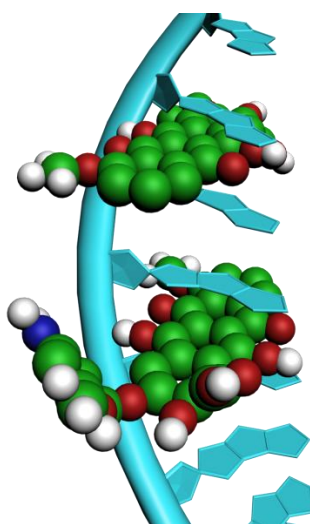

Figure 4. Simple scheme of interaction of doxorubicin with ssDNA. Most likely, the interactions can be expected between doxorubicin and adenine and/or guanosine.

GL4. CA peak decreased for more than 30 % (1:1(-♦-)), for more than 60 % (1:2(-x-)) and for more than 70 % (1:5(-■-)) in the beginning of incubation. CA peak enhanced with the increasing time of incubation (Fig. 5A), which is very similar to ssODN GL6. There were determined also similar trends in DOXO peak heights, i.e. height increased with the increasing time of incubation. However, GL4 sequence showed the growth signal in ratios of 1:5 and 1:1. Ratio 1:2 was nearly constant over time. The signal at a given time increased in the following sequence 1:2 < 1:1 < 1:5. In the case of ssODN CA3 and MT5, a strong decrease of the CA peak but not very significant increase in signal doxorubicin were determined (Figs. 5C, D). **CA3.** This ssODN sequence provided the decreasing CA peak for all ratios within the range from 0 to 45 minutes with the fact that ratio of 1:5 had the lowest drop in signal level compared to the reference signal. This is very interesting phenomenon, because aforementioned sequences had very distinct behaviour. This clearly relates with the effect of primary structure of ssODNs. Up to 150 min., CA peak increased, then decreased (240 min.), and then there was a slight increase of the CA signal (Fig. 5A). CA3 sequence provided a well-differentiated according to individual ratio. The signal at a given time increased in the following sequence 1:2 < 1:1 < 1:5 (Fig. 5C). **MT5.** This sequence provided increasing CA peak for all ratios within the range from 0 to 45 minutes with the fact that ratios of 1:2 and 1:5 had very similar dependencies.
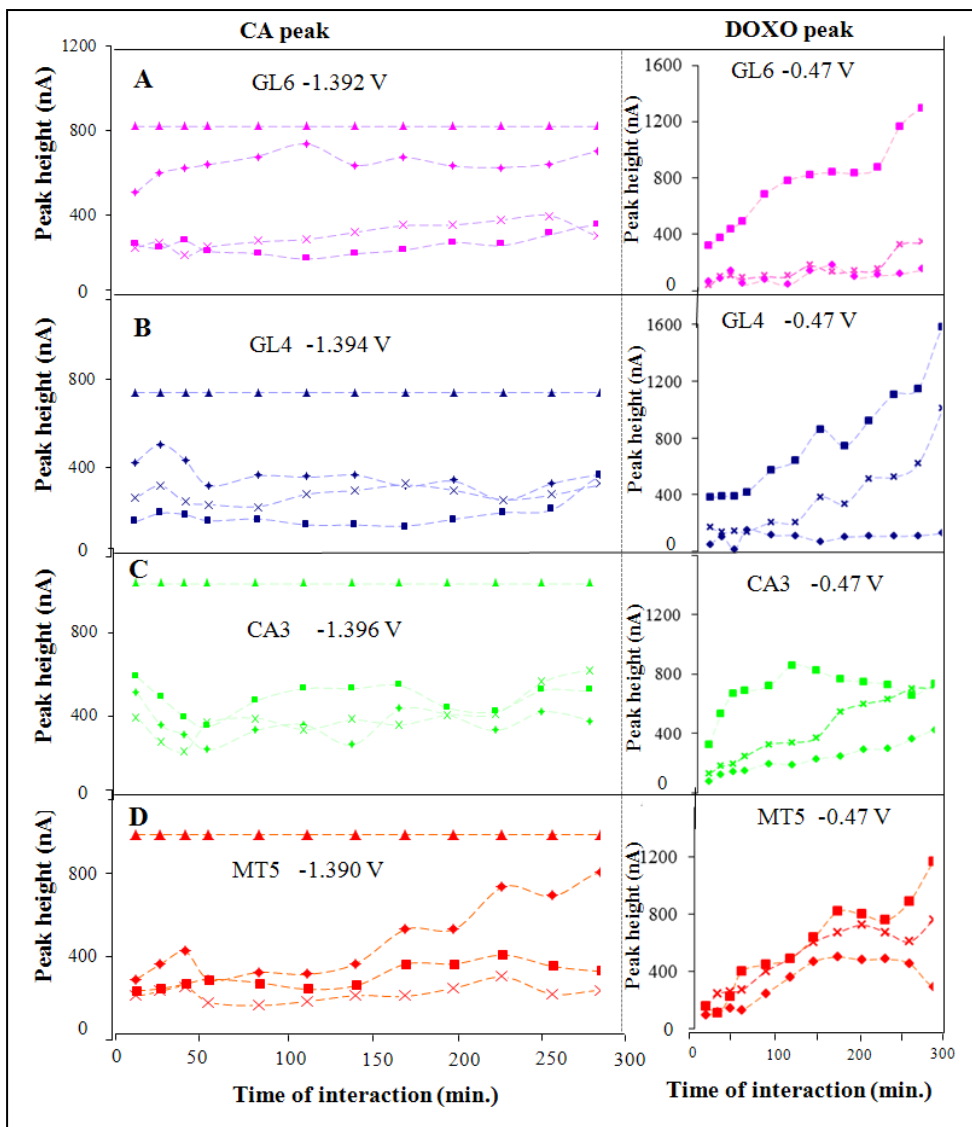
Figure 5. Time of interaction dependence (0 - 300 min) of CA peak height (position: -1.393 V) and DOXO peak height (position: -0.470 V) for the following ratios 1:1(-♦-), 1:2(-x-) and 1:5(-■-) of oligonucleotide:doxorubicin. Reference (-▲-) is average height of CA peaks of studied dsODNs without doxorubicin (n = 10). Interaction was carried out in thermomixer at 400 rpm, 25 °C. For other experimental details see Fig. 1.

At higher incubation times, the measured dependencies were well differentiated. The highest decrease in signal compared to reference level showed the ratio of 1:2. CA peak measured at ratio 1:1 increased with the increasing time of cultivation up to nearly 90 % of the reference signal (Fig. 5D). MT5 sequence has at least differentiated time series for the individual ratios of a mixture of doxorubicin with oligonucleotide. The signal at a given time increased in the following sequence 1:2 < 1:5 < 1:1 (Fig. 5D). Effect of ODN sequence on the observed electrochemical behaviour is not clear and will require further detailed research. Based on the obtained it is clear that there is an interaction of doxorubicin with ssODN. It is likely that there is a change in the electron transport of DNA [86] and other structural changes.

CA and DOX peaks were correlated in the following part of this study and are summarized in Figs. 6, 7 and 8 for ratios of 1:1, 1:2 and 1:5, respectively. The reference peak of CA is indicated by a 100 % (red circle). Percentage change in the height of CA peak in a mixture of oligonucleotide-doxorubicin was related to the reference value of the peak size of the oligonucleotide itself. Percentage change in peak height of DOXO in a mixture of oligonucleotide-doxorubicin was related to the maximum peak height a given time dependence. The figures were plotted with the following times of incubation 30, 150, 240 and 300 min. A mixture of oligonucleotide-doxorubicin mixed in a 1:1 ratio provided the correlated results, which are shown in Fig. 6. There is shown a horizontal time sequence of points (the lowest values for 30 min interaction, while the highest value for 300 minutes long interaction). It is obvious that CA3 sequence had the strongest doxorubicin intercalation (CA3 points in the diagram are shifted to the most left, decrease the size of the signal oligonucleotide is the highest). The lowest value of the interaction shows a sequence GL6, which is on the right side in the figure (decrease in the size of the signal oligonucleotide is lowest). MT5 sequence shows decrease in CA peak to 37 % of the reference signal up to 150 min. interaction and then increase to 75 % at 240 min. and 81 % at 300 min. The intensity of the signal of GL4 decreased with increasing time of interaction (Fig. 6).
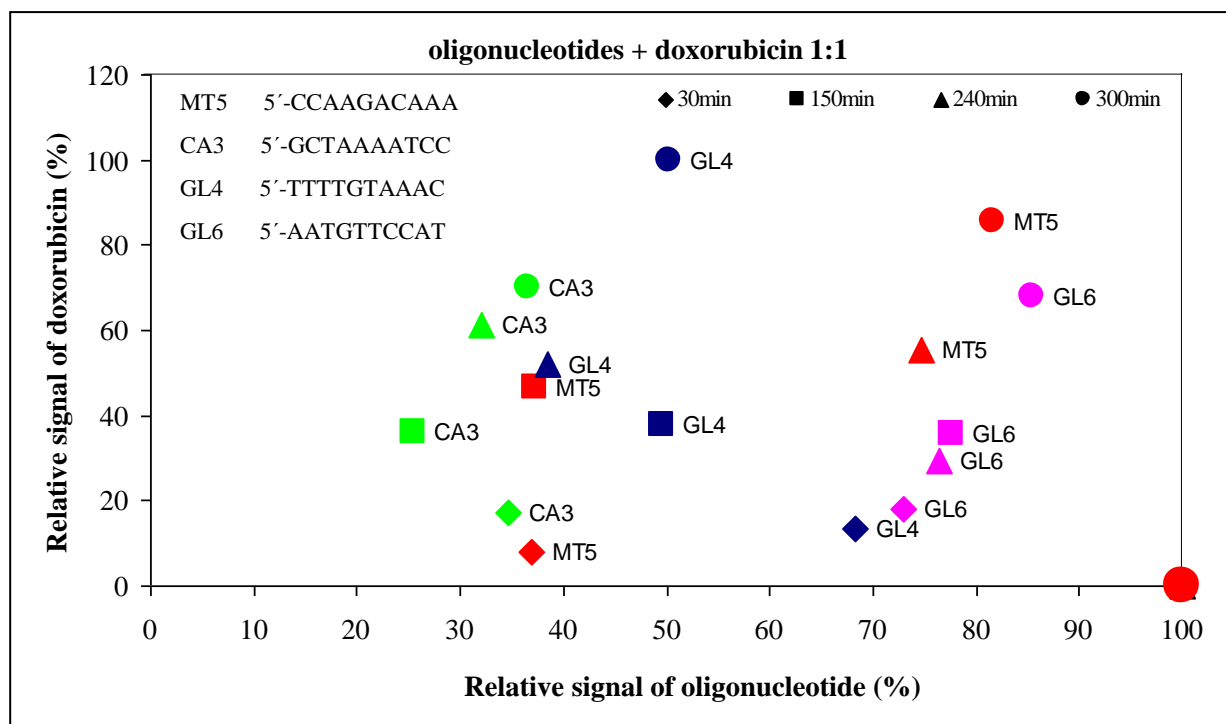

Figure 6. Relative signal of doxorubicin as a function of relative signal of oligonucleotide in ratio 1:1 (oligonucleotide:doxorubicin). Time dependence (30, 150, 240 and 300 min.) for four types of oligonucleotides is presented (MT5, CA3, GL4 and GL6). Relative signal of doxorubicin is relative to maximum value of one time series for each rate. Relative signal of oligonucleotide is relative to average value of signal of pure oligonucleotide. dsODN concentration 0.5 µg/ml and doxorubicin concentration 0.5 µg/ml. All experiments were carried out in triplicates. The biggest red dot indicates reference CA peak height. For other experimental details see Fig. 1.

A mixture of oligonucleotide-doxorubicin mixed in a 1:2 ratio behave in a slightly different form (Fig. 7). Compared with the ratio of 1:1 (Fig. 6) it is observed a marked decrease in CA peak and increase in DOXO peak (shift to the left part of the figure). Horizontal chronology is not as well differentiated, there is horizontal mixing time dependencies for each interaction. At this ratio the strongest interaction between doxorubicin and ssODN was observed in MT5, which ranges between 22-30 % of peak height of the reference value in the whole time manner. CA3 sequence shows a linear decrease in the intensity of interaction with the value of reliability $R^2 = 0.96$. The decline starts at 25 % and ends at 60 % of the reference signal. Sequence GL4 and GL6 interact most strongly at 30 min (16-18%) and then the intensity of interaction decreases, and at 300 min. has a value of 44 % and 37 %, respectively.

The most significant changes in signals were observed in the ratio 1:5. Mixture ssODN-doxorubicin mixed in the ratio of 1:5 showed decrease after 30 min. interaction for 20-30 % for all studied ssODNs. At the time of 150 min., the intensity did not change, except for CA3 sequence. At the time of 300 min., the intensity of all sequences varied within the interval from 40 to 50 %, except MT5 sequence, which shows a decrease to 33 %. At this ratio, there is a strong decrease in the CA signal peaks (marked shift to the left in this figure), however the peak height of CA and DOXO increased with increasing interaction time (Fig. 8).
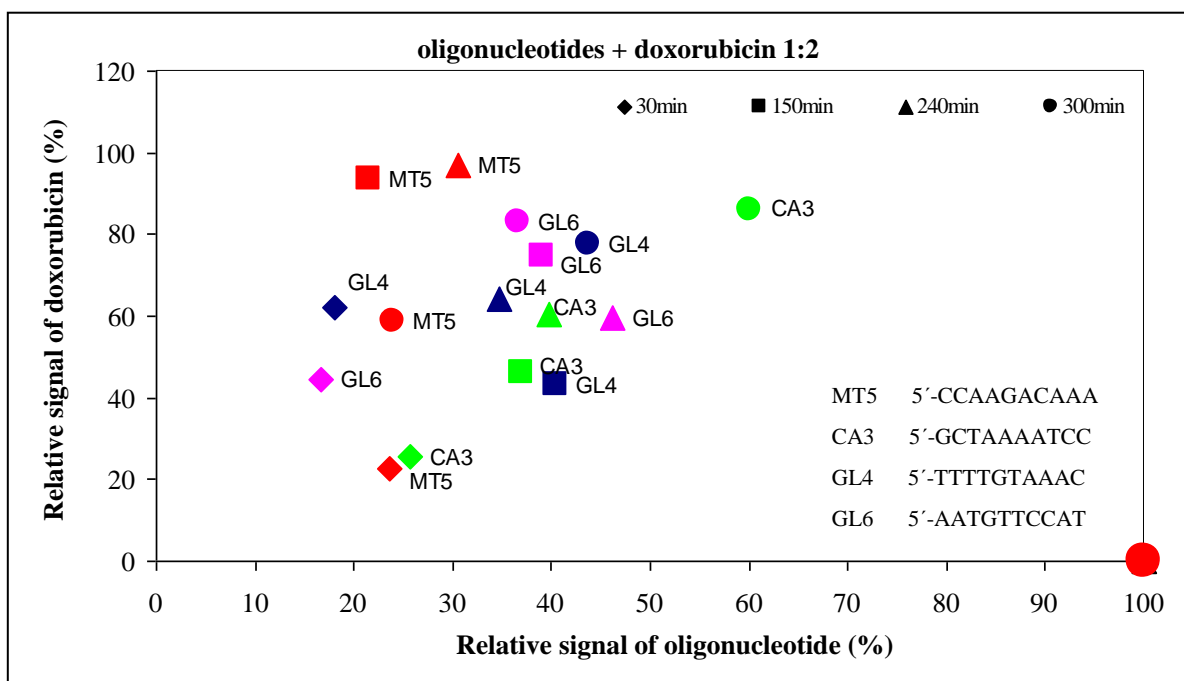

Figure 7. Relative signal of doxorubicin as a function of relative signal of oligonucleotide in ratio 1:2 (oligonucleotide:doxorubicin). Time dependence (30, 150, 240 and 300 min.) for four types of oligonucleotides is presented (MT5, CA3, GL4 and GL6). Relative signal of doxorubicin is relative to maximum value of one time series for each rate. Relative signal of oligonucleotide is relative to average value of signal of pure oligonucleotide. dsODN concentration 0.5 µg/ml and doxorubicin concentration 1 µg/ml. All experiments were carried out in triplicates. The biggest red dot indicates reference CA peak height. For other experimental details see Fig. 1.
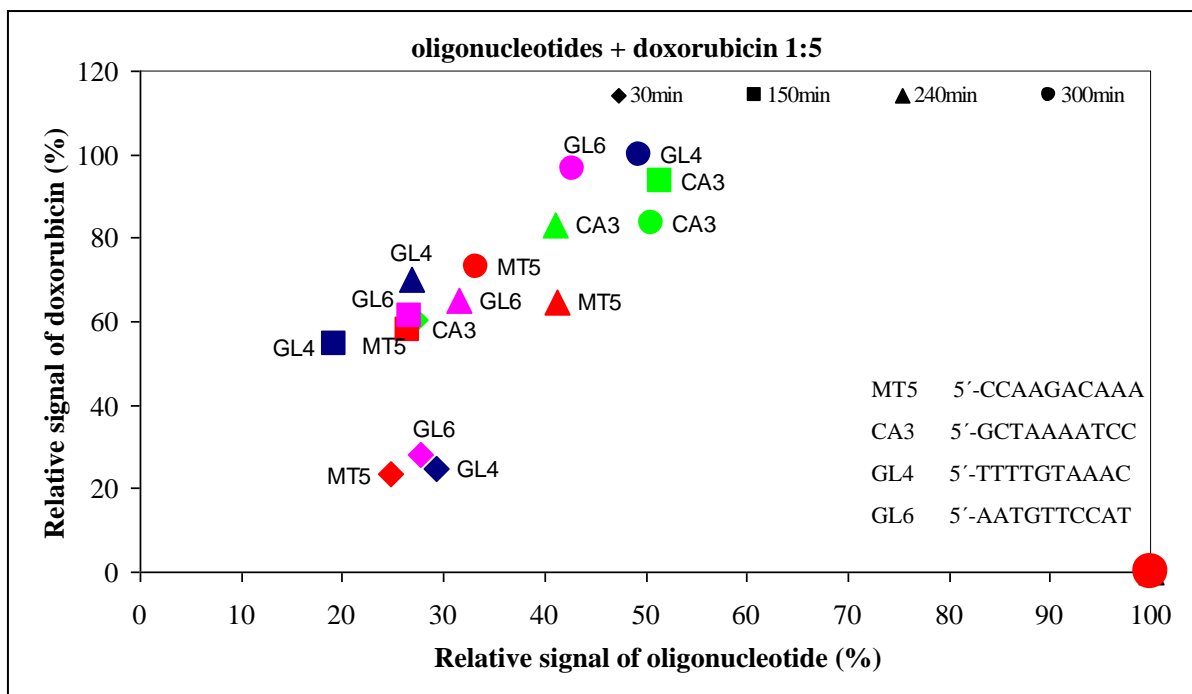
Figure 8. Relative signal of doxorubicin as a function of relative signal of oligonucleotide in ratio 1:5 (oligonucleotide:doxorubicin). Time dependence (30, 150, 240 and 300 min.) for four types of oligonucleotides is presented (MT5, CA3, GL4 and GL6). Relative signal of doxorubicin is relative to maximum value of one time series for each rate. Relative signal of oligonucleotide is relative to average value of signal of pure oligonucleotide. dsODN concentration 0.5 µg/ml and doxorubicin concentration 2.5 µg/ml. All experiments were carried out in triplicates. The biggest red dot indicates reference CA peak height. For other experimental details see Fig. 1.

When comparing the results (Figs. 6, 7, 8) for three ratios of the mixture it is clear that the interval of peak intensities of oligonucleotide reduces with increasing ratio of oligonucleotide-doxorubicin, i.e. for ratio 1:1 it is 25-85 %, for ratio 1:2 it is 16-60 % and for ratio 1:5 it is 19-51 %. The interval of relative signal intensities of doxorubicin ranges from 8 to 100 % for ratio 1:1, 22-100 % for ratios 1:2 and 1:5. The results showed the assumption that DOXO peak height increased with increasing concentration of the drug intercalated into ssODN, but the signals CA peaks changes during the interaction suggest the changes in the structure of ssODN. Differences in interactions of DOXO with different ssODN allow to speculate that this cytostatic drug may have selective effect on some cancers with specific genetic changes especially gene amplifications.

4. CONCLUSIONS

Electrochemical analysis is suitable for monitoring the interaction of anticancer drug doxorubicin with ssODN. The results showed a clear interaction between doxorubicin and ssODN. In addition, significant differences are apparent in the observed CA and DOXO peaks depending on the sequence of ssODN. However, the explanation for this phenomenon is not easy and will probably be

associated with changes of electron conductivity of DNA and other structural changes in individual ssODNs.

References

1. G. P. Risbridger, I. D. Davis, S. N. Birrell and W. D. Tilley, *Nat. Rev. Cancer*, 10 (2010) 205.
2. S. Di Cosimo and J. Baselga, *Nat. Rev. Clin. Oncol.*, 7 (2010) 139.
3. S. X. Lin, J. Chen, M. Mazumdar, D. Poirier, C. Wang, A. Azzi and M. Zhou, *Nat. Rev. Endocrinol.*, 6 (2010) 485.
4. U. Capitanio and N. Suardi, *Nat. Rev. Urol.*, 8 (2011) 65.
5. N. Lawrentschuk and L. Klotz, *Nat. Rev. Urol.*, 8 (2011) 312.
6. S. F. Oon, S. R. Pennington, J. M. Fitzpatrick and R. W. G. Watson, *Nat. Rev. Urol.*, 8 (2011) 131.
7. V. Brabec and J. Kasparkova, *Drug Resist. Update*, 5 (2002) 147.
8. V. Brabec and J. Kasparkova, *Drug Resist. Update*, 8 (2005) 131.
9. L. Kelland, *Nat. Rev. Cancer*, 7 (2007) 573.
10. J. Petrlova, D. Potesil, J. Zehnalek, B. Sures, V. Adam, L. Trnkova and R. Kizek, *Electrochim. Acta*, 51 (2006) 5169.
11. V. Supalkova, M. Beklova, J. Baloun, C. Singer, B. Sures, V. Adam, D. Huska, J. Pikula, L. Rauscherova, L. Havel, J. Zehnalek and R. Kizek, *Bioelectrochemistry*, 72 (2008) 59.
12. D. Huska, I. Fabrik, J. Baloun, V. Adam, M. Masarik, J. Hubalek, A. Vasku, L. Trnkova, A. Horna, L. Zeman and R. Kizek, *Sensors*, 9 (2009) 1355.
13. C. Palmieri, J. Krell, C. R. James, C. Harper-Wynne, V. Misra, S. Cleator and D. Miles, *Nat. Rev. Clin. Oncol.*, 7 (2010) 561.
14. R. Kizek, V. Adam, J. Hrabeta, T. Eckschlager, S. Smutny, J. V. Burda, E. Frei and M. Stiborova, *Pharmacol. Ther.*,133(2012) 26.
15. G. Minotti, P. Menna, E. Salvatorelli, G. Cairo and L. Gianni, *Pharmacol. Rev.*, 56 (2004) 185.
16. K. Kiyomiya, S. Matsuo and M. Kurebe, *Cancer Chemother. Pharmacol.*, 47 (2001) 51.
17. V. G. S. Box, *J. Mol. Graph.*, 26 (2007) 14.
18. H. G. Keizer, H. M. Pinedo, G. J. Schuurhuis and H. Joenje, *Pharmacol. Ther.*, 47 (1990) 219.
19. P. K. Singal and N. Iliskovic, *N. Engl. J. Med.*, 339 (1998) 900.
20. R. R. Patil, S. A. Guhagarkar and P. V. Devarajan, *Crit. Rev. Ther. Drug Carr. Syst.*, 25 (2008) 1.
21. C. F. Thorn, C. Oshiro, S. Marsh, T. Hernandez-Boussard, H. McLeod, T. E. Klein and R. B. Altman, *Pharmacogenet. Genom.*, 21 (2011) 440.
22. F. Patolsky, E. Katz and I. Willner, *Angew. Chem.-Int. Edit.*, 41 (2002) 3398.
23. H. Berg, G. Horn, H. E. Jacob, U. Fiedler, U. Luthardt and D. Tresselt, *Bioelectrochem. Bioenerg.*, 16 (1986) 135.
24. J. Wang, M. S. Lin and V. Villa, *Analyst*, 112 (1987) 1303.
25. J. B. Hu, Q. Q. Huang and Q. L. Li, *Chin. Sci. Bull.*, 46 (2001) 1355.
26. K. Hashimoto, K. Ito and Y. Ishimori, *Anal. Chim. Acta*, 286 (1994) 219.
27. D. Abd El-Hady, M. I. Abdel-Hamid, M. M. Seliem and N. A. El-Maali, *Talanta*, 66 (2005) 1207.
28. D. Huska, V. Adam, J. Hubalek, L. Trnkova, T. Eckschlager, M. Stiborova, I. Provaznik and R. Kizek, *Chim. Oggi-Chem. Today*, 28 (2010) 18.

29. D. Huska, V. Adam, S. Krizkova, J. Hrabeta, T. Eckschlager, M. Stiborova and R. Kizek, *Chim. Oggi-Chem. Today*, 28 (2010) 15.
30. S. Eynollahi, S. Riahi, M. R. Ganjali and P. Norouzi, *Int. J. Electrochem. Sci.*, 5 (2010) 1367.
31. T. R. R. Naik and H. S. B. Naik, *Int. J. Electrochem. Sci.*, 3 (2008) 409.
32. S. Riahi, S. Eynollahi, M. R. Ganjali and P. Norouzi, *Int. J. Electrochem. Sci.*, 5 (2010) 1151.
33. S. Riahi, S. Eynollahi, M. R. Ganjali and P. Norouzi, *Int. J. Electrochem. Sci.*, 5 (2010) 815.
34. S. Riahi, S. Eynollahi, M. R. Ganjali and P. Norouzi, *Int. J. Electrochem. Sci.*, 5 (2010) 355.
35. J. Vacek, L. Havran and M. Fojta, *Collect. Czech. Chem. Commun.*, 74 (2009) 1727.
36. Y. H. Hahn and H. Y. Lee, *Arch. Pharm. Res.*, 27 (2004) 31.
37. D. Abd El-Hady, M. I. Abdel-Hamid, M. M. Seliem and N. A. E-Maali, *Arch. Pharm. Res.*, 27 (2004) 1161.
38. S. M. Golabi and D. Nematollahi, *J. Pharm. Biomed. Anal.*, 10 (1992) 1053.
39. H. M. Zhang and N. Q. Li, *J. Pharm. Biomed. Anal.*, 22 (2000) 67.
40. J. Vacek, L. Havran and M. Fojta, *Electroanalysis*, 21 (2009) 2139.
41. S. Krizkova, V. Adam, J. Petrlova, O. Zitka, K. Stejskal, J. Zehnalek, B. Sures, L. Trnkova, M. Beklova and R. Kizek, *Electroanalysis*, 19 (2007) 331.
42. R. P. Baldwin, D. Packett and T. M. Woodcock, *Anal. Chem.*, 53 (1981) 540.
43. S. Komorsky-Lovric and M. Lovric, *Collect. Czech. Chem. Commun.*, 72 (2007) 1398.
44. Y. Z. Fang, S. H. Liu and P. G. He, *Chem. J. Chin. Univ.-Chin.*, 17 (1996) 1222.
45. S. Komorsky-Lovric, *Bioelectrochemistry*, 69 (2006) 82.
46. Z. Jemelkova, J. Zima and J. Barek, *Collect. Czech. Chem. Commun.*, 74 (2009) 1503.
47. M. S. Ibrahim, Z. A. Ahmed, Y. M. Temerk and H. Berg, *Bioelectrochem. Bioenerg.*, 36 (1995) 149.
48. E. N. Chaney and R. P. Baldwin, *Anal. Chim. Acta*, 176 (1985) 105.
49. X. Chu, G. L. Shen, J. H. Jiang, T. F. Kang, B. Xiong and R. Q. Yu, *Anal. Chim. Acta*, 373 (1998) 29.
50. J. B. Hu and Q. L. Li, *Chin. Chem. Lett.*, 11 (2000) 601.
51. J. B. Hu, J. Shang and Q. L. Li, *Anal. Lett.*, 33 (2000) 1843.
52. M. Buckova, P. Grundler and G. U. Flechsig, *Electroanalysis*, 17 (2005) 440.
53. D. M. Gao, J. B. Hu, M. Yang and Q. L. Li, *Anal. Biochem.*, 358 (2006) 70.
54. D. P. dos Santos, M. F. Bergamini and M. V. B. Zanoni, *Int. J. Electrochem. Sci.*, 5 (2010) 1399.
55. A. Erdem and M. Ozsoz, *Electroanalysis*, 14 (2002) 965.
56. H. Y. Ma, L. P. Zhang, Y. Pan, K. Y. Zhang and Y. Z. Zhang, *Electroanalysis*, 20 (2008) 1220.
57. H. C. M. Yau, H. L. Chan and M. S. Yang, *Biosens. Bioelectron.*, 18 (2003) 873.
58. A. M. Oliveira-Brett, M. Vivan, I. R. Fernandes and J. A. P. Piedade, *Talanta*, 56 (2002) 959.
59. P. S. Guin, S. Das and P. C. Mandal, *J. Phys. Org. Chem.*, 23 (2010) 477.
60. J. A. Plambeck and J. W. Lown, *J. Electrochem. Soc.*, 131 (1984) 2556.
61. J. A. P. Piedade, I. R. Fernandes and A. M. Oliveira-Brett, *Bioelectrochemistry*, 56 (2002) 81.
62. R. Hajian, N. Shams and M. Mohagheghian, *J. Bras. chem. soc.*, 20 (2009) 1399.
63. D. Huska, V. Adam, P. Babula, J. Hrabeta, M. Stiborova, T. Eckschlager, L. Trnkova and R. Kizek, *Electroanalysis*, 21 (2009) 487.
64. D. Huska, V. Adam, J. Burda, J. Hrabeta, T. Eckschlager, P. Babula, R. Opatrilova, L. Trnkova, M. Stiborova and R. Kizek, *Febs J.*, 276 (2009) 109.
65. M. Masarik, H. Kynclova, D. Huska, J. Hubalek, V. Adam, P. Babula, T. Eckschlager, M. Stiborova and R. Kizek, *Int. J. Mol. Med.*, 26 (2010) S46.
66. R. Prusa, D. Huska, V. Adam, J. Kukacka, J. Hrabeta, T. Eckschlager, P. Babula, M. Stiborova, L. Trnkova and R. Kizek, *Clin. Chem.*, 55 (2009) A217.
67. M. Masarik, D. Huska, V. Adam, J. V. Burda, T. Eckschlager, M. Stiborova and R. Kizek, *Int. J. Mol. Med.*, 24 (2009) S49.

68. L. Trnkova, M. Stiborova, D. Huska, V. Adam, R. Kizek, J. Hubalek, T. Eckschlager and Ieee, Electrochemical biosensor for investigation of anticancer drugs interactions (doxorubicin and ellipticine) with DNA, 2009.
69. S. Cakir, E. Bicer, E. Coskun and O. Cakir, *Bioelectrochemistry*, 60 (2003) 11.
70. B. P. Ting, J. Zhang, Z. Q. Gao and J. Y. Ying, *Biosens. Bioelectron.*, 25 (2009) 282.
71. T. L. Liao, Y. F. Wang, X. B. Zhou, Y. Zhang, X. H. Liu, J. Du, X. J. Li and X. Q. Lu, *Colloid Surf. B-Biointerfaces*, 76 (2010) 334.
72. H. Jiang and X. M. Wang, *Electrochem. Commun.*, 11 (2009) 126.
73. S. F. Lu, *Anal. Lett.*, 36 (2003) 2597.
74. K. Y. Zhang and Y. Z. Zhang, *Microchim. Acta*, 169 (2010) 161.
75. W. Yan, X. C. Shen, Z. L. Zhang, C. Chen and D. W. Pang, *Anal. Lett.*, 38 (2005) 2579.
76. Y. H. Lu, X. Y. Yang, Y. F. Ma, Y. Huang and Y. S. Chen, *Biotechnol. Lett.*, 30 (2008) 1031.
77. X. Y. Yang, X. Y. Zhang, Z. F. Liu, Y. F. Ma, Y. Huang and Y. Chen, *J. Phys. Chem. C*, 112 (2008) 17554.
78. S. Tanaka, F. Yamamoto, K. Sugarwara and H. Nakamura, *Talanta*, 44 (1997) 357.
79. K. Sugawara, S. Tanaka and H. Nakamura, *Anal. Chem.*, 67 (1995) 299.
80. L. X. Gong, C. M. Wei, J. B. Hu and Q. L. Li, *Chin. J. Anal. Chem.*, 36 (2008) 1121.
81. J. J. Fei, X. Q. Wen, Y. Zhang, L. H. Yi, X. M. Chen and H. Cao, *Microchim. Acta*, 164 (2009) 85.
82. M. Song and X. Wang, *Electrochem. Solid State Lett.*, 10 (2007) F9.
83. G. C. Zhao and X. Yang, *Electrochem. Commun.*, 12 (2010) 300.
84. G. L. Long and J. D. Winefordner, *Anal. Chem.*, 55 (1983) A712.
85. J. C. Genereux and J. K. Barton, *Nat. Chem.*, 1 (2009) 106.
86. J. D. Slinker, N. B. Muren, S. E. Renfrew and J. K. Barton, *Nat. Chem.*, 3 (2011) 228.
87. C. E. Ashley, E. C. Carnes, G. K. Phillips, D. Padilla, P. N. Durfee, P. A. Brown, T. N. Hanna, J. W. Liu, B. Phillips, M. B. Carter, N. J. Carroll, X. M. Jiang, D. R. Dunphy, C. L. Willman, D. N. Petsev, D. G. Evans, A. N. Parikh, B. Chackerian, W. Wharton, D. S. Peabody and C. J. Brinker, *Nat. Mat.*, 10 (2011) 389.
88. S. Casares, A. C. Stan, C. A. Bona and T. D. Brumeanu, *Nat. Biotechnol.*, 19 (2001) 142.
89. J. A. MacKay, M. N. Chen, J. R. McDaniel, W. G. Liu, A. J. Simnick and A. Chilkoti, *Nat. Mat.*, 8 (2009) 993.
90. D. Huska, V. Adam, L. Trnkova and R. Kizek, *Chem. Listy*, 104 (2010) 177.
91. D. Huska, J. Hubalek, V. Adam and R. Kizek, *Electrophoresis*, 29 (2008) 4964.
92. D. Huska, J. Hubalek, V. Adam, D. Vajtr, A. Horna, L. Trnkova, L. Havel and R. Kizek, *Talanta*, 79 (2009) 402.
93. R. Prusa, J. Kukacka, D. Vajtr, D. Huska, J. Alba, V. Adam and R. Kizek, *Clin. Chem.*, 54 (2008) A156.
94. R. Mikelova, L. Trnkova, F. Jelen, J. Hubalek, V. Adam, R. Kizek and Ieee, in 2006 Ieee Sensors, Vols 1-3, 2006, p. 1143.
95. D. Huska, V. Adam, L. Trnkova and R. Kizek, *J. Magn. Magn. Mater.*, 321 (2009) 1474.
96. T. Vojtylova, D. Dospivova, O. Triskova, I. Pilarova, P. Lubal, M. Farkova, L. Trnkova and P. Taborsky, *Chem. Pap.*, 63 (2009) 731.
97. R. Mikelova, L. Trnkova and F. Jelen, *Electroanalysis*, 19 (2007) 1807.
98. L. Trnkova, F. Jelen and I. Postbieglova, *Electroanalysis*, 18 (2006) 662.
99. L. Trnkova, I. Postbieglova and M. Holik, *Bioelectrochemistry*, 63 (2004) 25.
100. D. Hynek, L. Krejcova, O. Zitka, V. Adam, L. Trnkova, J. Sochor, M. Stiborova, J. Hubalek, T. Eckschlager and R. Kizek, *Int. J. Electrochem. Sci.*, 8 (2011) in press.